Chapter 6

Sonochemical Degradation of Perfluorooctane Sulfonate (PFOS) and Perfluorooctanoate (PFOA) in Landfill Groundwater: Environmental Matrix Effect*

6.1 Abstract

Perfluorinated chemicals such as perfluorooctane sulfonate (PFOS) and perfluorooctanoic acid (PFOA) are environmentally persistent and recalcitrant to most conventional chemical and microbial treatment technologies. In this chapter, we show that sonolysis is able to decompose PFOS and PFOA present in groundwater beneath a landfill. However, the pseudo-first-order rate constant for the sonochemical degradation in the landfill groundwater is reduced by 61% and 56% relative to Milli-Q water for PFOS and PFOA, respectively, primarily due to the presence of other organic constituents. In this study, we evaluate the effect of various organic compounds on the sonochemical decomposition rates of PFOS and PFOA. Organic components in environmental matrices may reduce the sonochemical degradation rates of PFOS and PFOA by competitive adsorption onto the bubble-water interface or by lowering the average interfacial temperatures during transient bubble collapse events. The effect of individual organic compounds depends on the Langmuir adsorption constant, the Henry's law constant, the specific heat capacity, and the overall endothermic heat of dissociation. Volatile organic compounds (VOCs) are identified as the primary cause of the sonochemical rate reduction for PFOS and PFOA in landfill groundwater, whereas the effect of dissolved natural organic matter (DOM) is not significant. Finally, a combined process of ozonation and sonolysis is shown to substantially recover the rate loss for PFOS and PFOA in landfill groundwater.

6.2 Introduction

Perfluorooctane sulfonate (PFOS) and perfluorooctanoate (PFOA) have been found to be widespread in the environment due to their persistence and the long-range atmospheric and oceanic transport of their precursors such as perfluoroalkyl sulfonamides (PFASs) and fluorotelomer alcohols (FTOHs).[1-3] PFOS and PFOA have been measured in most natural waters from non-detectable to ng L^{-1} levels,[4-6] whereas higher concentrations (up to 2300 and 6570 μg L^{-1} for PFOS and PFOA, respectively) have been measured in groundwater collected from military bases where aqueous film-forming foams (AFFF) are used for fire-training activities.[7] Recently, PFOS and PFOA, together with other perfluorinated chemicals, have been detected in groundwater emanating from disposal sites in the Minneapolis/St. Paul area.[8] In addition, PFOS and PFOA have been detected in wildlife [9-11] as well as in human blood serum,[12] seminal plasma,[13] and breast milk.[14]

The presence of PFOS and PFOA has initiated efforts to develop effective water treatment technologies. Both compounds are recalcitrant to most conventional chemical and microbial treatment schemes.[15,16] It was found in a wastewater treatment process that in some cases the mass flows of PFOS and PFOA could increase as a result of precursor degradation.[16,17] Advanced oxidation processes (AOPs) are also ineffective for treating PFOS and PFOA due to their relatively slow reaction rates with OH radicals.[18] Wastewater containing perfluorochemicals can potentially be treated by activated carbon adsorption, reverse osmosis (RO), or nanofiltration (NF).[19,20] Nevertheless, the removal efficiency may be significantly impaired by other components in the wastewater matrix.[19,20] On the other hand, treating PFOS and PFOA at lower concentrations present in natural waters presents certain challenges. Various treatment techniques have been

evaluated, such as UV photolysis,[21,22] reduction by elemental iron,[23] and acoustic cavitation,[24] but to our knowledge, none have been tested on environmental samples.

Sonochemical degradation is effective in treating PFOS and PFOA present in aqueous solution over a wide range of concentrations.[25] Acoustic cavitation induced by high-frequency ultrasonic irradiation of aqueous solutions produces transient high temperatures in the bubble vapor phase and at the bubble-water interface. Because of their high surface activity, PFOS and PFOA preferentially partition to the bubble-water interface, where temperatures are on the order of 1000 K during a transient bubble collapse,[26] and are thus decomposed via *in situ* pyrolysis. Following the initial rate-limiting pyrolysis step, PFOS and PFOA are rapidly converted to CO, CO_2, fluoride (F^-), and sulfate (SO_4^{2-}). A sonochemical degradation half-life under 30 minutes has been reported for both PFOS and PFOA.[25] In addition, the sonochemical degradation rates are observed to increase linearly with increasing acoustic power density, and scaling-up the reactor size has minimal effect on reaction rates,[27] thus making sonochemical degradation a promising treatment method for PFOS and PFOA.

Previous studies on the sonochemical decomposition of PFOS and PFOA have focused on pure aqueous solutions. It is of practical interest to examine this process in environmentally relevant matrices, as the various matrix components may significantly affect the sonochemical kinetics and therefore the overall treatment efficiency. In this chapter, we determined the sonochemical kinetics of PFOS and PFOA present in the groundwater beneath a landfill. In addition, landfill groundwater components including volatile organic compounds (VOCs) and dissolved natural organic matter (DOM) were evaluated individually with respect to their effect on sonochemical degradation rates.

Finally, the sonozone process, i.e., sonolysis combined with ozonation, was applied in an attempt to enhance the degradation rates of PFOS and PFOA in the landfill groundwater. Results from this study can be used to estimate the matrix effect on the sonochemical degradation rates of PFOS and PFOA in various environmental media and to design remediation strategies accordingly.

6.3 Experimental Methods

***Materials*.** Ammonium perfluorooctanoate (APFO) and potassium perfluorooctane sulfonate (PFOS-K^+) standards were provided by 3M. Methanol, acetone, isopropyl alcohol, methyl-t-butyl-ether (MTBE), ethyl acetate, toluene, p-xylene, m-xylene, ethyl benzene, methyl isobutyl ketone (MIBK), and ammonium acetate were obtained from EMD chemicals. Suwannee River humic and fulvic acid standards were purchased from International Humic Substances Society. Sep-Pak Vac tC18 (6 cc, 1 g) solid phase extraction (SPE) cartridges were purchased from Waters. Purified water (18.2 MΩ cm^{-1} resistivity) was prepared using the Millipore Milli-Q Gradient water purification system.

Sonolysis. Sonications were performed in a 600 mL jacketed glass reactor at a frequency of 354 or 612 kHz using an Allied Signal–ELAC Nautik ultrasonic transducer. The applied power density was 250 W L^{-1} with an average energy-transfer efficiency of 72% as measured by calorimetry. The solutions were maintained at 10 ºC by water cooling and sparged with argon 30 minutes prior to and during the course of the reaction. In sonozone experiments, an ozone/oxygen gaseous mixture (2.5% v/v ozone) produced by an Orec V10-0 corona ozone generator was sparged into the reaction solution at 0.5 L min^{-1}. In all experiments the initial concentrations of both PFOS and PFOA were approximately 100 μg L^{-1}.

Solid phase extraction. Landfill groundwater samples taken during the sonochemical reactions were purified by SPE using Sep-Pak Vac tC18 cartridges (6 cc, 1 g) to remove matrix components that may interfere with the LC/MS analysis. The SPE cartridges were conditioned by passing 10 mL methanol and 50 mL water through the cartridges at a flow rate of 2 mL min^{-1}. The analytical samples were subsequently loaded onto the wet cartridges at 1 mL min^{-1}. The columns were dried with nitrogen gas for 5 minutes, rinsed with 10 mL 20% methanol in water at 2 mL min^{-1}, and dried with nitrogen gas for another 30 minutes. The analytes were eluted with methanol at 1 mL min^{-1}, and 4.0 mL samples were collected into 14 mL polypropylene tubes (Falcon). Sample aliquots (700 μL) were transferred to HPLC vials (Agilent) for the LC/MS analysis. All steps except sample loading were performed on a Caliper AutoTrace SPE Work Station.

LC/MS analyses. The concentrations of PFOS and PFOA were quantified by LC/MS. Sample aliquots (700 μL) were withdrawn from the reactor using disposable plastic syringes, transferred into 750 μL polypropylene autosampler vials, and sealed with PTFE septum crimp caps (Agilent). 20 μL of samples were injected into an Agilent 1100 HPLC for separation on a Thermo-Electron Betasil C18 column (100 mm × 2.1 mm, 5 μm). An identical guard column was placed in front of the analytical column. The flow rate was maintained at 0.3 mL min^{-1} with a mobile phase of 2 mM ammonium acetate in water (A) and methanol (B). The eluent gradient started with 5% B over the first minute, was ramped to 90% B over 10 minutes and held for 2.5 minutes, then ramped back to 5% B over 0.5 minutes and held for 3 minutes, and finished with a 3 minute post time. Chromatographically separated samples were analyzed by an Agilent Ion Trap in negative mode monitoring for the perfluorooctanesulfonate molecular ion (m/z = 499)

and the decarboxylated perfluorooctanoate (*m/z* = 369). Instrumental parameters were set at the following levels: nebulizer pressure 40 PSI, drying gas flow rate 9 L min^{-1}, drying gas temperature 325 ºC, capillary voltage +3500 V, and skimmer voltage –15 V. Quantification was based on a 8-point calibration curve spanning the 1 to 200 μg L^{-1} range fitted to a quadratic with X^{-1} weighting. Analytical standards, quality control, and reagent blank samples were included in each analytical batch along with the unknown samples. Further analytical details were described in Table 6.3 and Figure 6.10, and in a previous paper (*25*).

Surface tension measurements. The surface tension of sample solutions was determined by a du Nouy interfacial tensiometer using the standard ring method (ASTM D1331-89).

6.4 Experimental Results

Groundwater characterization. The groundwater used in this study was sampled from beneath a landfill located within the city of Oakdale, MN, and therefore contains organic chemicals that are also present in the landfill. As summarized in Table 6.1, the landfill groundwater has a total organic carbon (TOC) concentration of 20 mg L^{-1}, primarily volatile organic compounds (VOCs) such as acetone, diisopropyl ether, and 2-butanone at mg L^{-1} levels. It also contains a moderately high level of bicarbonate and iron. The concentrations of PFOS and PFOA in the landfill groundwater are 30 and 65 μg L^{-1}, respectively.

Sonolysis of PFOS and PFOA- Matrix Effects. The sonochemical degradation kinetics of PFOS and PFOA ($[PFOS]_i = [PFOA]_i$ = 100 μg L^{-1}) in landfill groundwater and Milli-Q water are shown in Figure 6.1. Sonolysis was performed under the following

conditions: ultrasonic frequency set at 354 or 612 kHz, applied power density set at a constant 250 W L^{-1}, and temperature maintained at 10 °C under an argon atmosphere. PFOS and PFOA were spiked into the groundwater to increase the concentration to 100 μg L^{-1} each. The sonochemical degradation of groundwater PFOS and PFOA follows pseudo first-order kinetics as is observed in Milli-Q, which agrees with the hypothesis that the initial decomposition mechanism remains the same. However, at 354 kHz, the first-order rate constant for the sonolysis of groundwater PFOS, k_{GW}^{-PFOS} = 0.0094 min^{-1}, is 39% of the Milli-Q rate constant, k_{MQ}^{-PFOS} = 0.024 min^{-1}. Similar results are observed for PFOA, where the rate constant for groundwater PFOA, k_{GW}^{-PFOA} = 0.021 min^{-1}, is 44% of the Milli-Q rate constant, k_{MQ}^{-PFOA} = 0.047 min^{-1}. At a sonolytic frequency of 612 kHz, a similar reduction in rate constant is observed when comparing sonolysis in Milli-Q versus in groundwater (Figure 6.7).

In order to probe the organic chemical species present in the landfill groundwater that are the most responsible for the reduction in sonochemical degradation rates, representative organic compounds were individually added to the aqueous solution of PFOS and PFOA, and their effect on the sonochemical degradation rates of PFOS and PFOA evaluated under the same sonolytic conditions as used in the previous experiments. Figure 6.2 shows the effect of methanol, acetone, isopropyl alcohol, ethyl acetate, and MTBE on the sonochemical degradation rates of PFOS and PFOA. In all cases, two regimes are observed with respect to the decrease in the sonochemical degradation rates as a function of increasing organic concentrations. The sonochemical degradation rate constant gradually decreases at relatively low organic concentrations, but above an

organic-specific threshold concentration, the decrease in rate constant shifts to a much steeper slope.

The effect of larger organic compounds such as toluene, ethyl benzene, p-xylene, m-xylene, and MIBK was also evaluated. At 10^{-4} mol L^{-1}, no significant effect on the sonochemical degradation rates is observed (Figure 6.3), but at 10^{-3} mol L^{-1}, MIBK reduces the sonochemical degradation rates of PFOA and PFOS by 46% and 66%, respectively. The effect of MIBK is greater than any of the five organic compounds in Figure 6.2. For the other four larger compounds, no higher concentrations were tested due to their low water solubilities.

In addition to VOCs, the effect of DOM on the sonochemical kinetics of PFOS and PFOA was also examined. DOM is composed of heterogeneous organic compounds including humic and fulvic acids. As is shown in Figure 6.4, no significant difference is found between the sonochemical degradation kinetics of PFOS and PFOA in Milli-Q water, a 15 mg L^{-1} humic acid solution, and a 15 mg L^{-1} fulvic acid solution. 15 mg L^{-1} represents the highest concentration of DOM found in most natural waters.

Sonozone treatment of PFOS and PFOA. We evaluated the performance of sonozone, a process that combines ozonation and sonolysis, on the degradation of PFOS and PFOA in landfill groundwater. As Figure 6.5 shows, by continuously sparging an oxygen/ozone mix gas (2.5% v/v O_3) during the course of sonolysis, the degradation rates are increased to 0.019 min^{-1} for PFOS and 0.033 min^{-1} for PFOA. This is equal to 79% and 70% of the Milli-Q rate constant for PFOS and PFOA, respectively. In comparison, replacing argon with either oxygen or an oxygen/ozone mix gas has no significant effect on the sonochemical kinetics of PFOS and PFOA in Milli-Q water (Figure 6.8).

6.5 Discussion

Based on the observation of two distinct regimes as shown in Figure 6.2, we propose that two different mechanisms are active in reducing the sonochemical degradation rates of PFOS and PFOA. The first mechanism is competitive adsorption onto the bubble-water interface by organic compounds other than PFOS and PFOA, which reduces the number of active surface sites available for PFOS and PFOA pyrolysis. The second mechanism is evaporation of the volatile organic compounds into the bubble vapor phase, which reduces the bubble vapor and interfacial temperatures during transient bubble collapse events by increasing the specific heat capacity of the bubble vapor and subsequent endothermic dissociation of these organic vapors.[28]

The two mechanisms are further elucidated by examining the mathematical expression for the sonochemical degradation rates of PFOS and PFOA. Assuming that competitive adsorption is active at the bubble-water interface, and that interfacial pyrolysis is the only viable degradation pathway for PFOS and PFOA, the sonochemical degradation rate of PFOX (PFOX denotes PFOS or PFOA) can be expressed as [29]

$$\frac{d[PFOX]}{dt} = -k_{app}^{-PFOX}[PFOX] = -k_{\Delta}^{-PFOX}\theta^{PFOX} \tag{6.1}$$

where k_{app}^{-PFOX} is the apparent pseudo first-order rate constant, k_{Δ}^{-PFOX} the maximum absolute rate attained when all of the transiently cavitating bubble surface sites are occupied by PFOX molecules, and θ^{PFOX} the fraction of PFOX molecules at the bubble-water interface in the presence of other organic compounds. k_{Δ}^{-PFOX} is given by

$$k_{\Delta}^{-PFOX} = [S]A^{PFOX}\exp\left(-E_A^{PFOX}/R\left\langle T_{\text{int}}^{bub}\right\rangle\right) \tag{6.2}$$

where $[S]$ is the molarity of bubble adsorption sites, A^{PFOX} and E_A^{PFOX} are the pre-exponential constant and activation energy for the initial PFOX pyrolysis, respectively, and $\left\langle T_{\text{int}}^{bub} \right\rangle$ is the average interfacial temperature during the high-temperature period of a transient bubble collapse. θ^{PFOX}, in the presence of other organic compounds competing for bubble interfacial sites, is given by

$$\theta^{PFOX} = \frac{K_L^{PFOX}[PFOX]}{1 + K_L^{PFOX}[PFOX] + \sum_i K_L^{org,i}[Org,i]} \tag{6.3}$$

where K_L^X is the Langmuir adsorption constant for compound X in L mol^{-1}. The K_L values for the five organic compounds in Figure 6.2 can be obtained from the surface tension curves shown in Figure 6.6. Least square fitting of the surface tension curves $\gamma(c)$'s to the Szyszkowski equation (Eq. (6.4)), the surface equation of state for the Langmuir isotherm (Eq. (6.5)), yields K_L as well as $\Gamma_{\max}$, the maximum surface concentration, for these five compounds (Table 6.2).

$$\Pi = \gamma_0 - \gamma(c) = nRT\Gamma_{\max} \ln(1 + K_L c) \tag{6.4}$$

$$\Gamma = \Gamma_{\max} \frac{K_L c}{1 + K_L c} \tag{6.5}$$

In Eq. (6.4), Π is the surface pressure in N m^{-1}, γ_0 = 0.072 N m^{-1} is the surface tension of pure water and $\gamma(c)$ is the surface tension of the aqueous solution of an organic compound at a given concentration c. As is shown in Table 6.2, $\Gamma_{\max}$ varies little among the five organic compounds, ranging from 4.7×10^{-6} to 8.2×10^{-6} mol m^{-2}. In contrast, K_L spans a much wider range from 3.9×10^{-4} m^3 mol^{-1} for methanol to around 1.9×10^{-2} m^3 mol^{-1} for ethyl acetate, which is about 50 times higher. Thus K_L is the key determining

factor for surface activity. According to Eq. (6.3), organic compounds with greater K_L values are more effective in reducing the sonochemical degradation rates of PFOS and PFOA by competitive adsorption onto the bubble-water interface. This trend is consistent with the experimental results shown in Figure 6.2.

As Eq. (6.2) suggests, another key driver for the sonochemical degradation rate of PFOS and PFOA is the average interfacial temperature during the high-temperature period of a transient bubble collapse. For example, considering that the activation energy for PFOA pyrolysis is E_A^{PFOA} = 172 kJ mol^{-1},[30] lowering $\left\langle T_{\text{int}}^{bub} \right\rangle$ from 1000 K to 900 K will reduce the reaction rate by 10 times. Volatile solutes such as alcohols are known to be able to significantly reduce the vapor and interfacial temperatures during bubble collapse.[28, 31, 32] The magnitude of the effect that an organic compound has on the bubble and interfacial temperatures is positively correlated with its Henry's law constant, its specific heat capacity, and its overall endothermic heat of dissociation. First, the Henry's law constant will determine the relative amount of solute that partitions to the bubble vapor phase during bubble expansion. Second, the presence of VOCs in the bubble vapor phase which have larger specific heat capacities than argon ($C_{p,Ar}$ = 20.8 J mol^{-1} K^{-1} at 298 K) will reduce the maximum bubble and interfacial temperatures achieved during bubble collapse. In addition, the organic compounds will be thermally decomposed under high temperatures inside the bubble, producing H_2, CO, and smaller organic compounds.[33-35] The endothermic dissociation of these compounds will further reduce bubble vapor and interfacial temperatures. Table 6.2 lists the Henry's law constants and the specific heat capacities at 298 K of the five organic compounds in Figure 6.2, and the values at a wider range of temperatures can be found in Figure 6.9. Although a complete

calculation of the overall heat of dissociation values taking into account all thermal reaction pathways is beyond the scope of this chapter, a positive correlation can be assumed between the overall heat of dissociation and the molecular size. The argument that VOCs affect the sonochemical kinetics by lowering the interfacial temperature is supported by the trend among the five organic compounds shown in Figure 6.2. The interfacial temperature reduction is also consistent with the observation that the groundwater matrix has a greater effect on the sonochemical degradation rate of PFOS than that of PFOA, since PFOS has a higher thermal activation energy.[36]

At concentrations up to 15 mg L^{-1}, neither humic nor fulvic acid has a significant effect on the sonochemical degradation rates of PFOS and PFOA. This suggests that neither of the aforementioned mechanisms is significant under these conditions. First, humic and fulvic acids are non-volatile and thus are expected to have little effect on the interfacial temperatures during bubble collapse. Second, though DOM is considered to be moderately surface active,[37] the effect of competitive adsorption onto the bubble-water interface is expected to be negligible at 15 mg L^{-1}. Given that the average molecular weight of DOM is at least 1 kDa [38] and that the average K_L value of DOM is arguably much smaller than $K_L^{PFOS} = 1.97$ m^3 mol^{-1} and $K_L^{PFOA} = 0.36$ m^3 mol^{-1},[29] the term $\sum_i K_L^{Org,i}[Org,i]$ in Eq. 6.3 is << 1, and thus negligible, at a DOM concentration of 15 mg L^{-1}.

Given the relatively low concentrations and surface activities of groundwater organic components evaluated in this study, competitive adsorption onto the bubble-water interface is expected to be of minor importance. However, this effect may be important in environmental matrices with higher concentrations of surface active components such as

aqueous film-forming foams (AFFF). The landfill groundwater in this study contains approximately 0.3 ~ 0.5 mmol L^{-1} VOCs, including larger and more volatile compounds such as diisopropyl ether and MIBK that are more effective than smaller VOCs (Figure 6.2) in reducing interfacial temperatures during bubble collapse. Therefore, temperature reduction by VOCs should be considered as the primary cause of the sonochemical rate reduction for PFOS and PFOA in the landfill groundwater. Inorganic components such as bicarbonate and sulfate ions may also contribute to the sonochemical rate reduction. In addition, adsorption of PFOS and PFOA onto organic matter and iron oxides in the landfill groundwater may reduce their concentrations at the bubble-water interface and therefore the degradation rates. However, the effect is not expected to be significant due to the relatively low partitioning coefficients of PFOS and PFOA.[39, 40]

The sonozone process is shown to significantly enhance the degradation rates of PFOS and PFOA in landfill groundwater, though it has no significant effect in Milli-Q water. The sonozone process has been shown to enhance the OH production rate.[35, 41, 42] Though reactions of OH radical with PFOS and PFOA are kinetically limited, OH radicals will react with VOCs present in the bubble vapor phase at a much faster rate than the thermal dissociation of these molecules and will increase their mineralization rates. The rapid destruction of VOCs will reduce their negative impact on interfacial temperatures during bubble collapse. The sonozone process shows potential for improving the degradation rates of PFOS and PFOA in landfill groundwater and other environmental media with high levels of VOCs.

6.6 Acknowledgements

The authors would like to thank 3M for the financial support and the Caltech Environmental Analysis Center (Dr. Nathan Dalleska) for technical assistance in sample analysis.

6.7 References

(1) Prevedouros, K.; Cousins, I. T.; Buck, R. C.; Korzeniowski, S. H., *Environ. Sci. Technol.* **2006,** *40*, 32-44.

(2) Ellis, D. A.; Martin, J. W.; De Silva, A. O.; Mabury, S. A.; Hurley, M. D.; Andersen, M. P. S.; Wallington, T. J., *Environ. Sci. Technol.* **2004,** *38*, 3316-3321.

(3) Shoeib, M.; Harner, T.; Vlahos, P., *Environ. Sci. Technol.* **2006,** *40*, 7577-7583.

(4) Yamashita, N.; Kannan, K.; Taniyasu, S.; Horii, Y.; Okazawa, T.; Petrick, G.; Gamo, T., *Environ. Sci. Technol.* **2004,** *38*, 5522-5528.

(5) So, M. K.; Taniyasu, S.; Yamashita, N.; Giesy, J. P.; Zheng, J.; Fang, Z.; Im, S. H.; Lam, P. K. S., *Environ. Sci. Technol.* **2004,** *38*, 4056-4063.

(6) Yamashita, N.; Kannan, K.; Taniyasu, S.; Horii, Y.; Petrick, G.; Gamo, T., *Mar. Pollut. Bull.* **2005,** *51*, 658-668.

(7) Schultz, M. M.; Barofsky, D. F.; Field, J. A., *Environ. Sci. Technol.* **2004,** *38*, 1828-1835.

(8) Minnesota Pollution Control Agency. *Investigation of Perfluorochemical (PFC) Contamination in Minnesota – Phase One*; Minnesota Pollution Control Agency, St. Paul, MN, 2006.

(9) Smithwick, M.; Mabury, S. A.; Solomon, K. R.; Sonne, C.; Martin, J. W.; Born, E. W.; Dietz, R.; Derocher, A. E.; Letcher, R. J.; Evans, T. J.; Gabrielsen, G. W.;

Nagy, J.; Stirling, I.; Taylor, M. K.; Muir, D. C. G., *Environ. Sci. Technol.* **2005,** *39*, 5517-5523.

(10) Sinclair, E.; Mayack, D. T.; Roblee, K.; Yamashita, N.; Kannan, K., *Arch. Environ. Contam. Toxicol.* **2006,** *50*, 398-410.

(11) Gulkowska, A.; Jiang, Q. T.; So, M. K.; Taniyasu, S.; Lam, P. K. S.; Yamashita, N., *Environ. Sci. Technol.* **2006,** *40*, 3736-3741.

(12) Yeung, L. W. Y.; So, M. K.; Jiang, G. B.; Taniyasu, S.; Yamashita, N.; Song, M. Y.; Wu, Y. N.; Li, J. G.; Giesy, J. P.; Guruge, K. S.; Lam, P. K. S., *Environ. Sci. Technol.* **2006,** *40*, 715-720.

(13) Guruge, K. S.; Taniyasu, S.; Yamashita, N.; Wijeratna, S.; Mohotti, K. M.; Seneviratne, H. R.; Kannan, K.; Yamanaka, N.; Miyazaki, S., *J. Environ. Monit.* **2005,** *7*, 371-377.

(14) So, M. K.; Yamashita, N.; Taniyasu, S.; Jiang, Q. T.; Giesy, J. P.; Chen, K.; Lam, P. K. S., *Environ. Sci. Technol.* **2006,** *40*, 2924-2929.

(15) Key, B. D.; Howell, R. D.; Criddle, C. S., *Environ. Sci. Technol.* **1998,** *32*, 2283-2287.

(16) Schultz, M. M.; Higgins, C. P.; Huset, C. A.; Luthy, R. G.; Barofsky, D. F.; Field, J. A., *Environ. Sci. Technol.* **2006,** 7350-7357.

(17) Sinclair, E.; Kannan, K., *Environ. Sci. Technol.* **2006,** *40*, 1408-1414.

(18) Schroder, H. F.; Meesters, R. J. W., *J. Chromatogr. A* **2005,** *1082*, 110-119.

(19) Tang, C. Y. Y.; Fu, Q. S.; Robertson, A. P.; Criddle, C. S.; Leckie, J. O., *Environ. Sci. Technol.* **2006,** *40*, 7343-7349.

(20) Tang, C. Y.; Fu, Q. S.; Criddle, C. S.; Leckie, J. O., *Environ. Sci. Technol.* **2007,** *41*, (6), 2008-2014.

(21) Hori, H.; Yamamoto, A.; Hayakawa, E.; Taniyasu, S.; Yamashita, N.; Kutsuna, S., *Environ. Sci. Technol.* **2005,** *39*, 2383-2388.

(22) Yamamoto, T.; Noma, Y.; Sakai, S. I.; Shibata, Y., *Environ. Sci. Technol.* **2007,** *41*, 5660-5665.

(23) Hori, H.; Nagaoka, Y.; Yamamoto, A.; Sano, T.; Yamashita, N.; Taniyasu, S.; Kutsuna, S.; Osaka, I.; Arakawa, R., *Environ. Sci. Technol.* **2006,** *40*, 1049-1054.

(24) Moriwaki, H.; Takagi, Y.; Tanaka, M.; Tsuruho, K.; Okitsu, K.; Maeda, Y., *Environ. Sci. Technol.* **2005,** *39*, 3388-3392.

(25) Vecitis, C. D., Park, H., Cheng, J., Mader, B. T., Hoffmann, M. R., *J. Phys. Chem. A* **2008,** *112*, 4261-4270

(26) Kotronarou, A.; Mills, G.; Hoffmann, M. R., *J. Phys. Chem.* **1991,** *95*, 3630-3638.

(27) Destaillats, H.; Lesko, T. M.; Knowlton, M.; Wallace, H.; Hoffmann, M. R., *Ind. Eng. Chem. Res.* **2001,** *40*, (18), 3855-3860.

(28) Yasui, K., *J. Chem. Phys.* **2002,** *116*, 2945-2954.

(29) Vecitis, C. D.; Park, H.; Cheng, J.; Mader, B. T.; Hoffmann, M. R., *J. Phys. Chem. A,* **2008**, 112, 16850-16857

(30) Krusic, P. J.; Roe, D. C., *Anal. Chem.* **2004,** *76*, 3800-3803.

(31) Ciawi, E.; Rae, J.; Ashokkumar, M.; Grieser, F., *J. Phys. Chem. B* **2006,** *110*, 13656-13660.

(32) Rae, J.; Ashokkumar, M.; Eulaerts, O.; von Sonntag, C.; Reisse, J.; Grieser, F., *Ultrason. Sonochem.* **2005,** *12*, 325-329.

(33) Anbar, M.; Pecht, I., *J. Phys. Chem.* **1964,** *68*, 1462-1465.

(34) Buttner, J.; Gutierrez, M.; Henglein, A., *J. Phys. Chem.* **1991,** *95*, 1528-1530.

(35) Kang, J. W.; Hoffmann, M. R., *Environ. Sci. Technol.* **1998,** *32*, 3194-3199.

(36) Glockner, V.; Lunkwitz, K.; Prescher, D., *Z. Tenside Surf. Det.* **1989,** *26*, 376-380.

(37) Ma, J.; Jiang, J.; Pang, S.; Guo, J., *Environ. Sci. Technol.* **2007,** *41*, 4959-4964.

(38) Perminova, I. V.; Frimmel, F. H.; Kudryavtsev, A. V.; Kulikova, N. A.; Abbt-Braun, G.; Hesse, S.; Petrosyan, V. S., *Environ. Sci. Technol.* **2003,** *37*, 2477-2485.

(39) Johnson, R. L.; Anschutz, A. J.; Smolen, J. M.; Simcik, M. F.; Penn, R. L., *J. Chem. Eng. Data.* **2007,** *52*, 1165-1170.

(40) Higgins, C. P.; Luty, R. G., *Environ. Sci. Technol.* **2007,** *41*, 3254-3261

(41) Weavers, L. K.; Ling, F. H.; Hoffmann, M. R., *Environ. Sci. Technol.* **1998,** *32*, 2727-2733.

(42) Lesko, T.; Colussi, A. J.; Hoffmann, M. R., *Environ. Sci. Technol.* **2006,** *40*, 6818-6823.

(43) Staudinger, J.; Roberts, P. V., *Chemosphere* **2001,** *44*, 561-576.

(44) Yaws, C. L. *Chemical Properties Handbook;* McGraw-Hill: New York, 1999.

Table 6.1. Primary components of the landfill groundwater [a]

pH	6.9-7.9	Dissolved Oxygen	2 mg L^{-1}
Temperature	10 – 15 ºC	TIC	40 mg L^{-1} C
TOC	20 mg L^{-1} C	$Fe_{(s)}$	30 mg L^{-1}
Acetone	7.15 mg L^{-1}	$Fe_{(aq)}$	5-8 mg L^{-1}
Diisopropyl Ether	3.54 mg L^{-1}	$Mn_{(s)}$	2 mg L^{-1}
MEK	3.37 mg L^{-1}	$Mn_{(aq)}$	0.5-1.6 mg L^{-1}
2-Propanol	2.47 mg L^{-1}	NH_4^+	0.2-0.6 mg L^{-1}
2-Butyl Alcohol	0.92 mg L^{-1}	SO_4^{2-}	4-30 mg L^{-1}
MIBK	0.55 mg L^{-1}	HS^-	0.2-0.5 mg L^{-1}

a. Measurements completed by Pace Analytical.

Table 6.2. Physical and thermodynamic properties of the five organic compounds in Figure 6.2

	$\Gamma_{max}\times10^{6}$ [a] (mol m^{-2})	K_L [b] (m^3 mol^{-1})	K_{iaw} [c]	$C_{p,g}$ [d] (J mol^{-1} K^{-1})
Methanol	8.2	3.9×10^{-4}	1.8×10^{-4}	45.2
Acetone	5.1	3.2×10^{-3}	1.4×10^{-3}	75.3
Isopropanol	4.8	7.8×10^{-3}	3.2×10^{-4}	90.0
Ethyl Acetate	4.7	1.9×10^{-2}	6.9×10^{-3}	117.5
MTBE	6.1	1.8×10^{-2}	2.6×10^{-2}	131.8
PFOS [e]	5.1	1.97	-	-
PFOA [e]	4.5	0.36	-	-

a. Γ_{max}, maximum surface concentration in Langmuir isotherm
b. K_L, Langmuir adsorption constant
c. K_{iaw}, Henry's law constant at 298 K , Reference 43
d. $C_{p,g}$, specific heat capacity at 298 K, Reference 44
e. Γ_{max} and K_L values for PFOS and PFOA listed for comparison, Reference 29

Table 6.3. Representative analytical results of quality-control samples

Standard concentration (ppb)	Average measurement (ppb) (n ≥ 4)	Standard deviation (%) (n ≥ 4)
PFOS		
10	9.5	3.3
25	24.1	5.8
50	53.3	2.3
100	104.3	4.6
PFOA		
10	9.6	6.9
25	26.5	3.7
50	51.4	3.7
100	106.1	3.4

Figure 6.1. $\ln([PFOS]_t / [PFOS]_i)$ (a) and $\ln([PFOA]_t / [PFOA]_i)$ (b) vs. time in minutes during sonochemical degradation in Milli-Q water (○) and landfill groundwater (□) under 354 kHz, 250 W L^{-1}, Ar, 10 ^oC for $[PFOS]_i = [PFOA]_i = 100$ μg L^{-1}. Each error bar represents one standard deviation from the mean of at least three experiments.

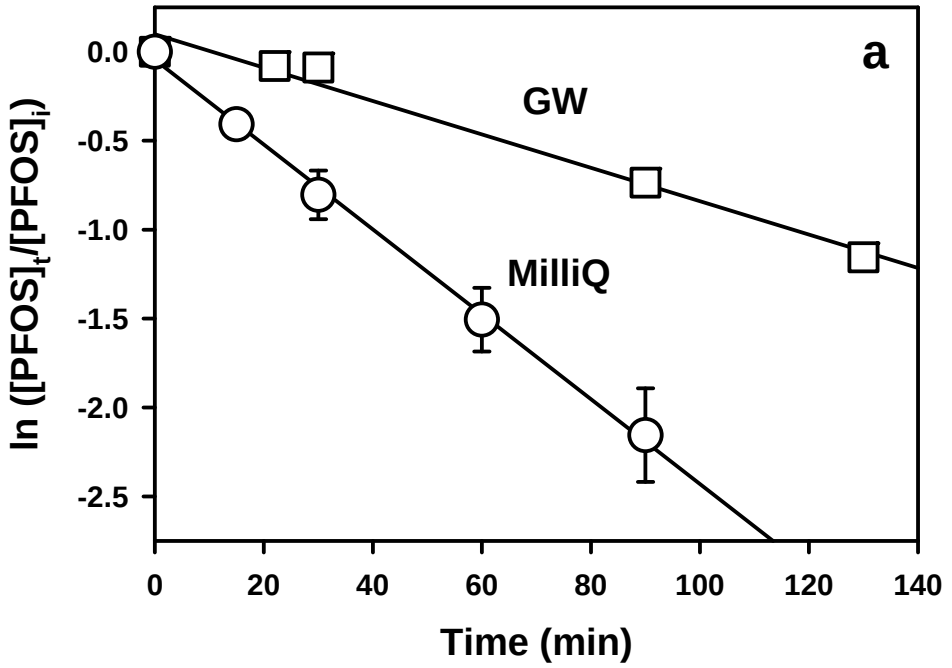

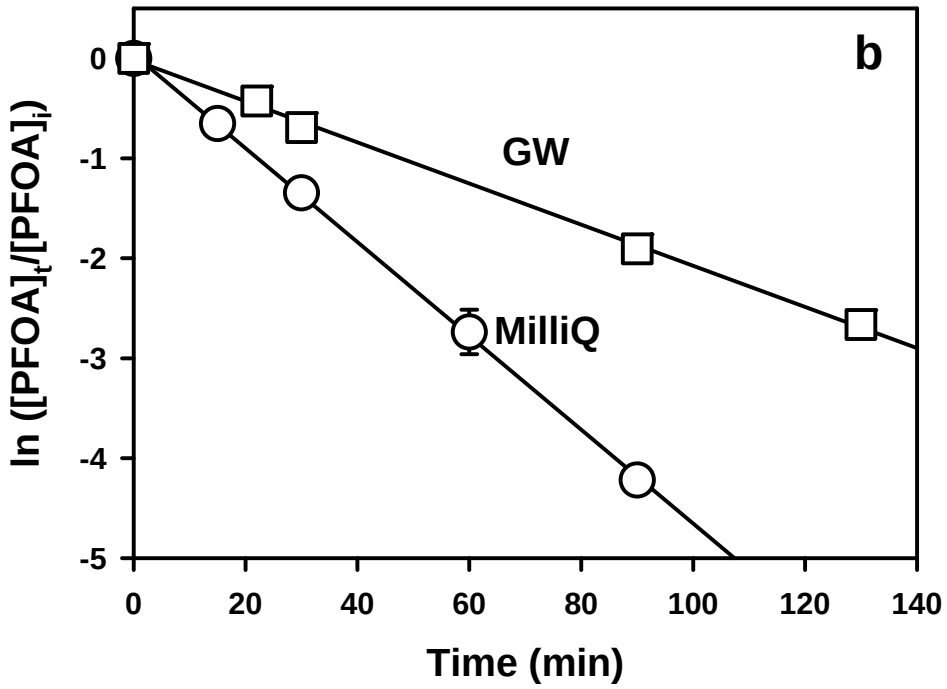

Figure 6.2. The observed pseudo first-order rate constant normalized to the Milli-Q rate constant, k^{-PFOS}/k_0^{-PFOS} (a) and k^{-PFOA}/k_0^{-PFOA} (b), vs. molar concentration of methanol (MeOH, ○), acetone (AC, ▽), isopropyl alcohol (IPA, □), ethyl acetate (EA, ◇), and MTBE (△) in aqueous solutions. The reaction conditions are: 354 kHz, 250 W L^{-1}, Ar, 10 °C, and $[PFOS]_i = [PFOA]_i = 100$ μg L^{-1}. Note that since the rate constant at 0.2 mol L^{-1} MTBE virtually drops to 0, the corresponding data point is not shown in the figure.

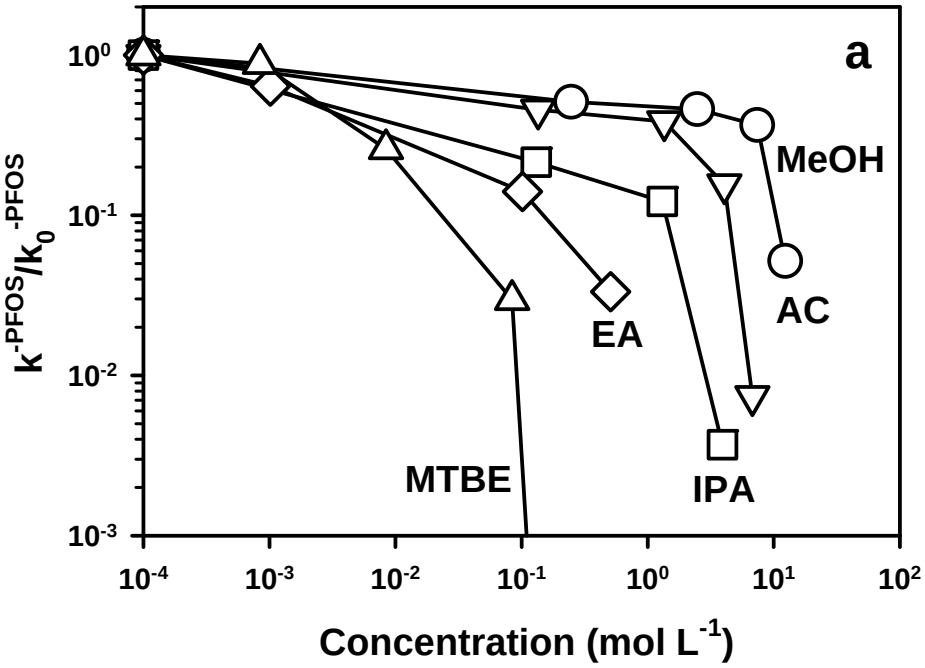

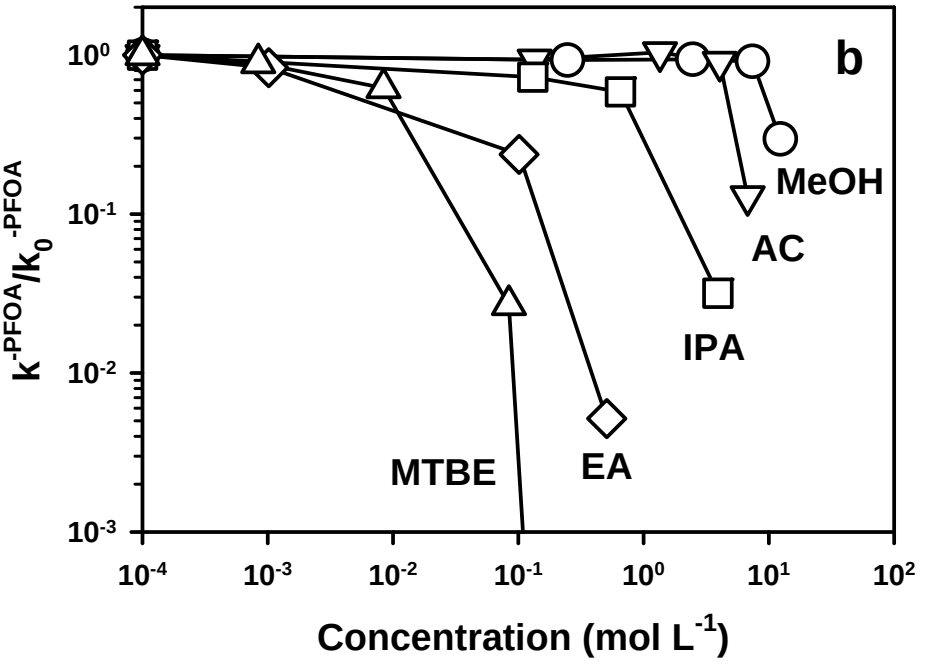

Figure 6.3. The pseudo-first-order rate constant for sonolysis of PFOA (clear bars) and PFOS (filled bars) in Milli-Q, 0.1 mM ethyl benzene (EB), 0.1 mM toluene (TL), 0.1 mM m-xylene (m-XL), 0.1 mM p-xylene (p-XL), 0.1 mM MIBK (MIBK), and 1 mM MIBK (MIBK*). The reaction conditions are 354 kHz, 250 W L^{-1}, Ar, 10 ^{o}C, $[PFOS]_i = [PFOA]_i = 100$ μg L^{-1}.

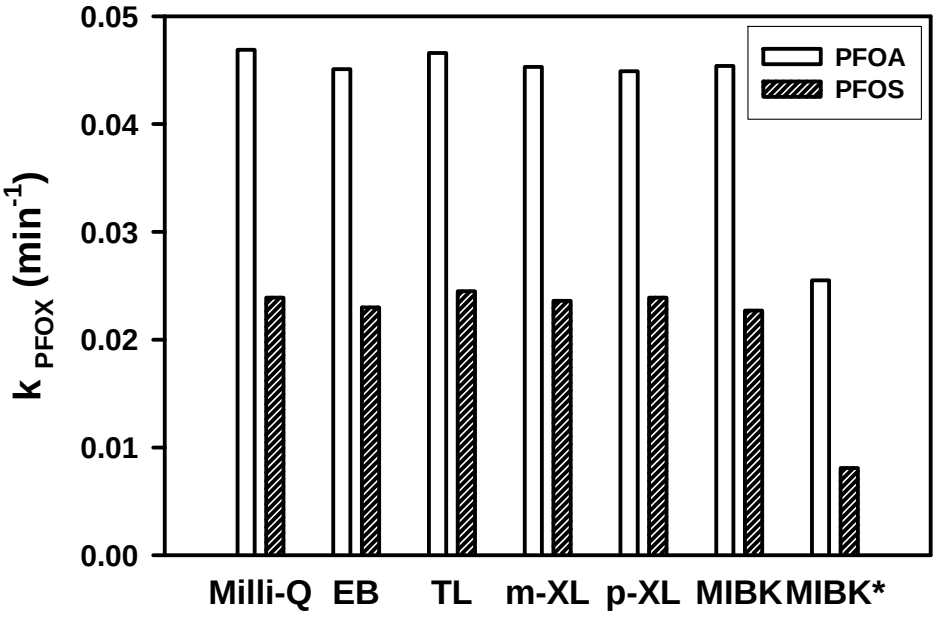

Figure 6.4 $\ln([PFOS]_t / [PFOS]_i)$ (a) and $\ln([PFOA]_t / [PFOA]_i)$ (b) vs. time in minutes during sonochemical degradation in Milli-Q water (○),15 mg L^{-1} humic acid solution (▽), and 15 mg L^{-1} fulvic acid solution (□) under 612 kHz, 250 W L^{-1}, Ar, 10 °C, for $[PFOS]_i = [PFOA]_i = 100$ μg L^{-1}.

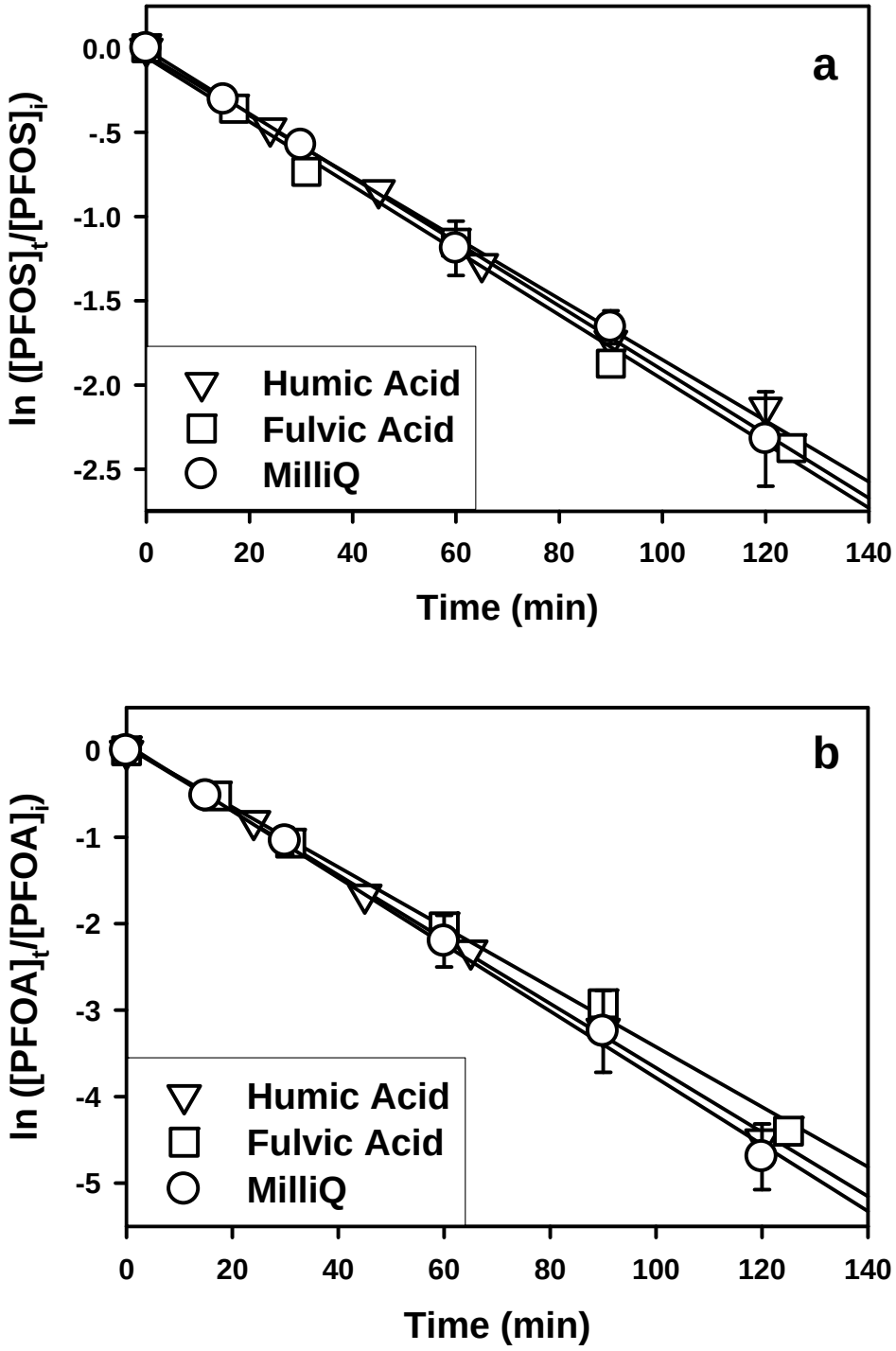

Figure 6.5. (a) $\ln([PFOS]_t / [PFOS]_i)$ and $\ln([PFOA]_t / [PFOA]_i)$ (b) vs. time in minutes during the sonolysis (○) and sonozone (▽) process of PFOS and PFOA in landfill groundwater. Sonochemical degradation kinetics in Milli-Q (□) are also included for comparison. Other reaction parameters are: 354 kHz, 250 W L^{-1}, Ar, 10 ^{o}C, and $[PFOS]_i = [PFOA]_i = 100$ μg L^{-1}.

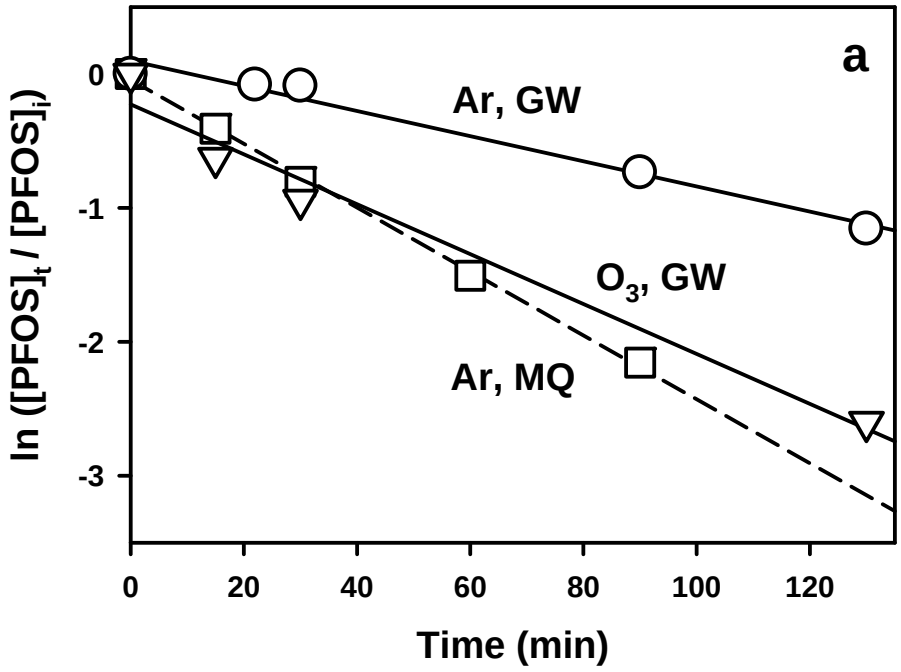

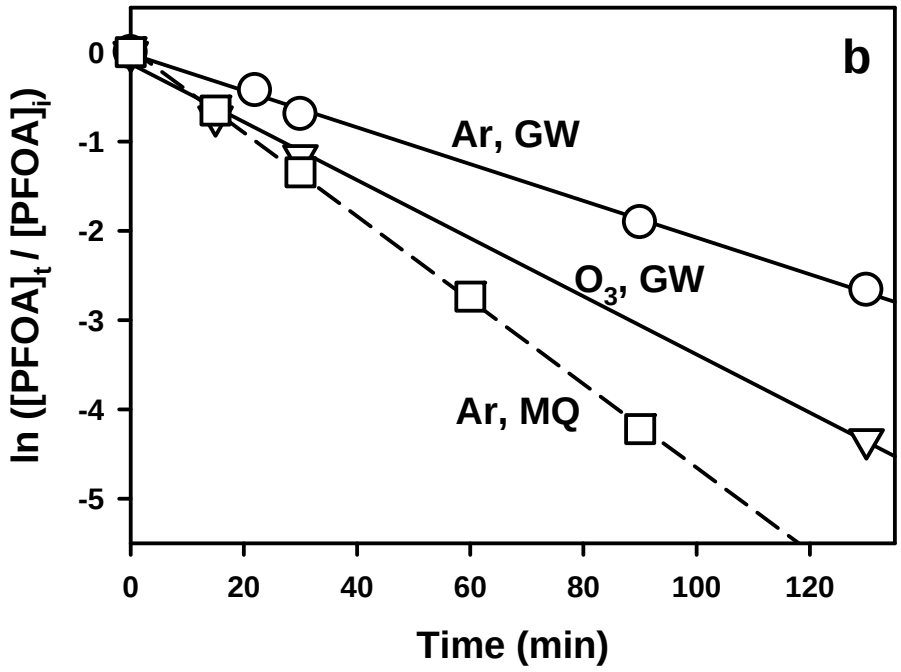

Figure 6.6. Surface tension vs. molar concentration of methanol (○), acetone (▽), isopropyl alcohol (□), ethyl acetate (◇), and MTBE (△) in aqueous solutions, measured at 298 K.

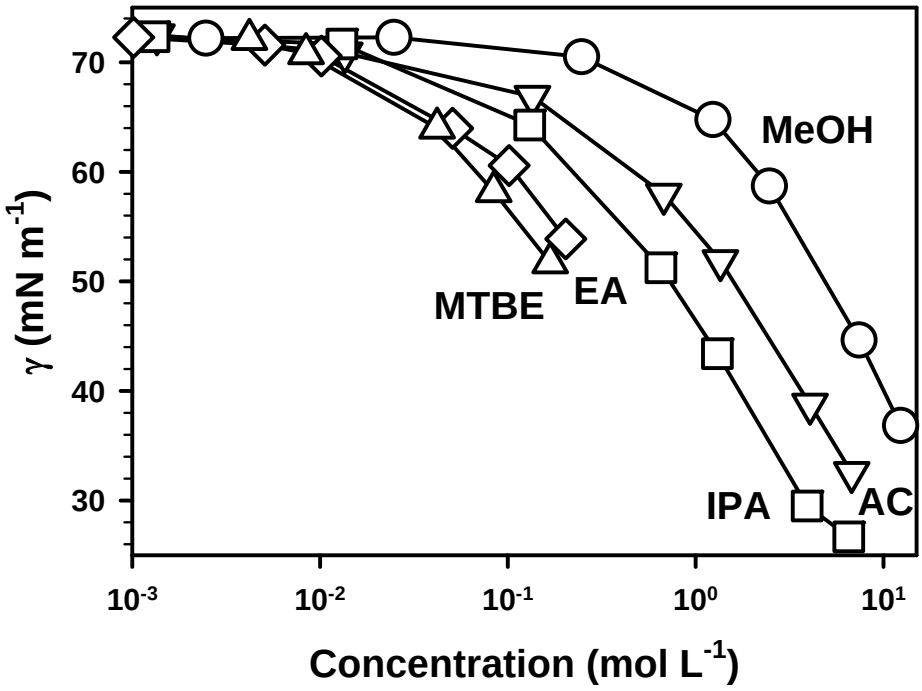

Figure 6.7. ln([PFOS]$_t$ / [PFOS]$_i$) (a) and ln([PFOA]$_t$ / [PFOA]$_i$) (b) vs. time in minutes during sonochemical degradation in Milli-Q water (○) and landfill groundwater (▽) under 612 kHz, 250 W L^{-1}, Ar, 10 ^{o}C for [PFOS]$_i$ = [PFOA]$_i$ = 100 μg L^{-1}.

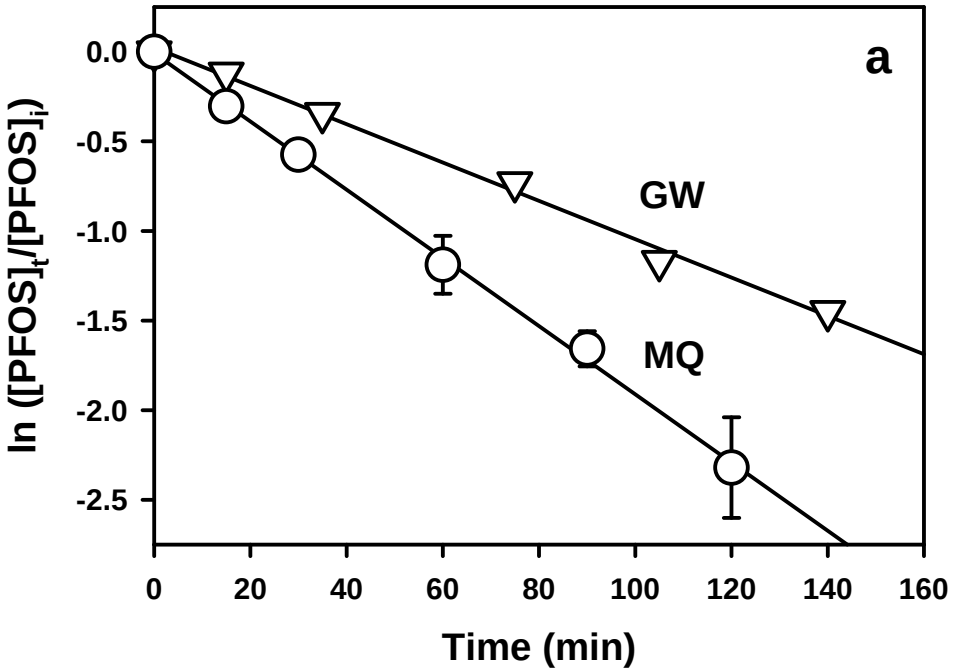

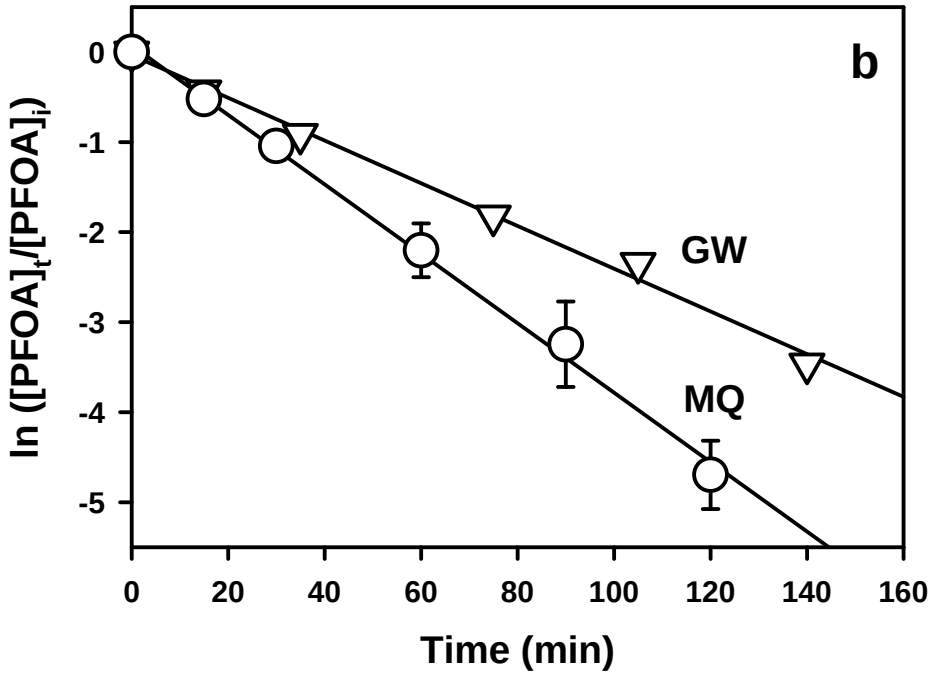

Figure 6.8. $\ln([PFOS]_t / [PFOS]_i)$ (a) and $\ln([PFOA]_t / [PFOA]_i)$ (b) vs. time in minutes during sonochemical degradation in Milli-Q water under Ar (○), O_2 (▽) and 2.5% O_3 in O_2 (□). Other reaction parameters are: 354 kHz, 250 W L^{-1}, 10 ^oC, and $[PFOS]_i = [PFOA]_i = 100$ μg L^{-1}.

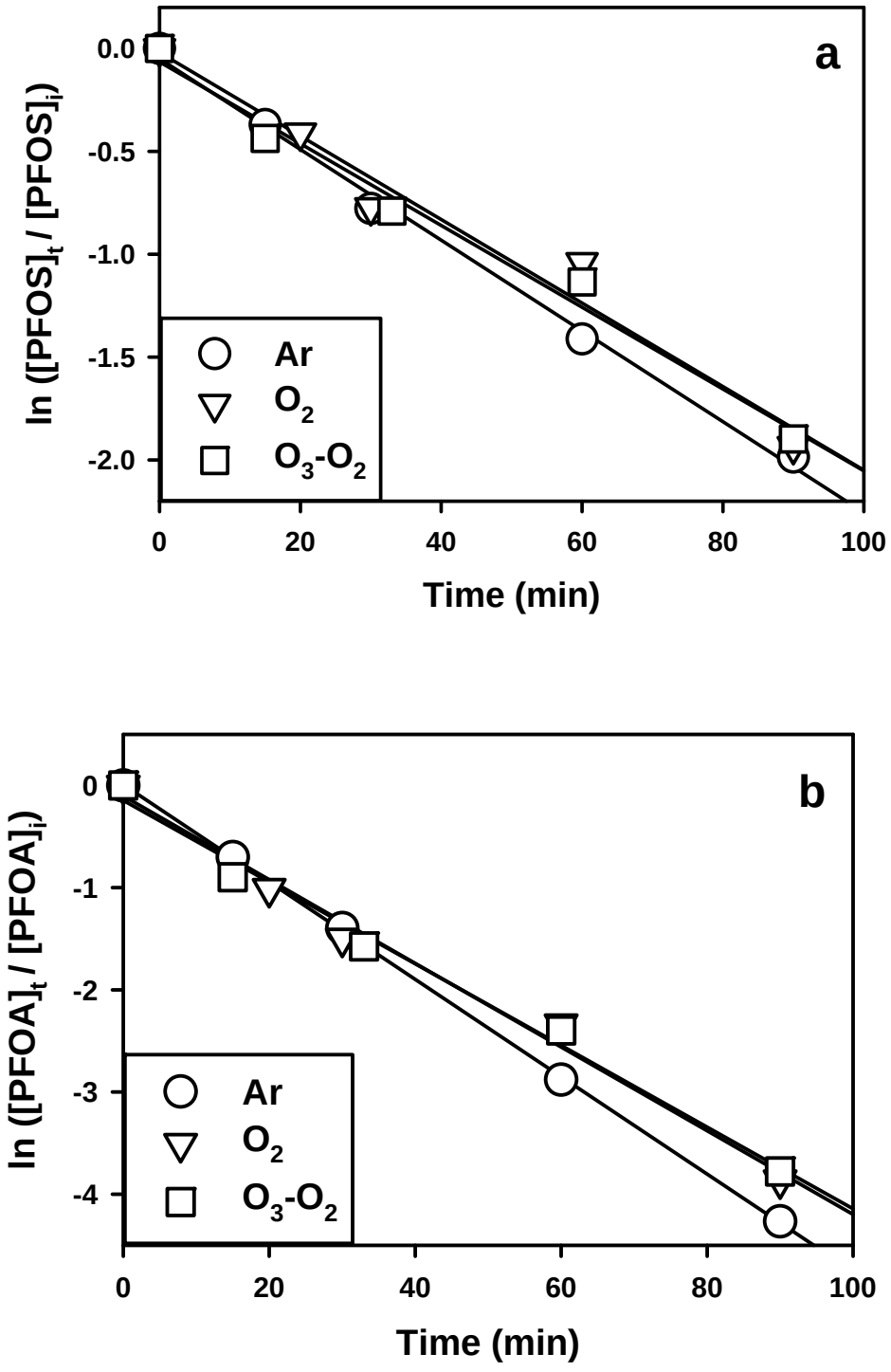

Figure 6.9. The gas phase specific heat capacity $C_{p,g}$ from T = 200 K to T = 1500 K (a), and the Henry's law constant k_{iaw} from T = 273 K to T = 373 K (b), for methanol (MeOH, ○), acetone (AC,▽), isopropyl alcohol (IPA, □), ethyl acetate (EA, ◇), and MTBE (△).

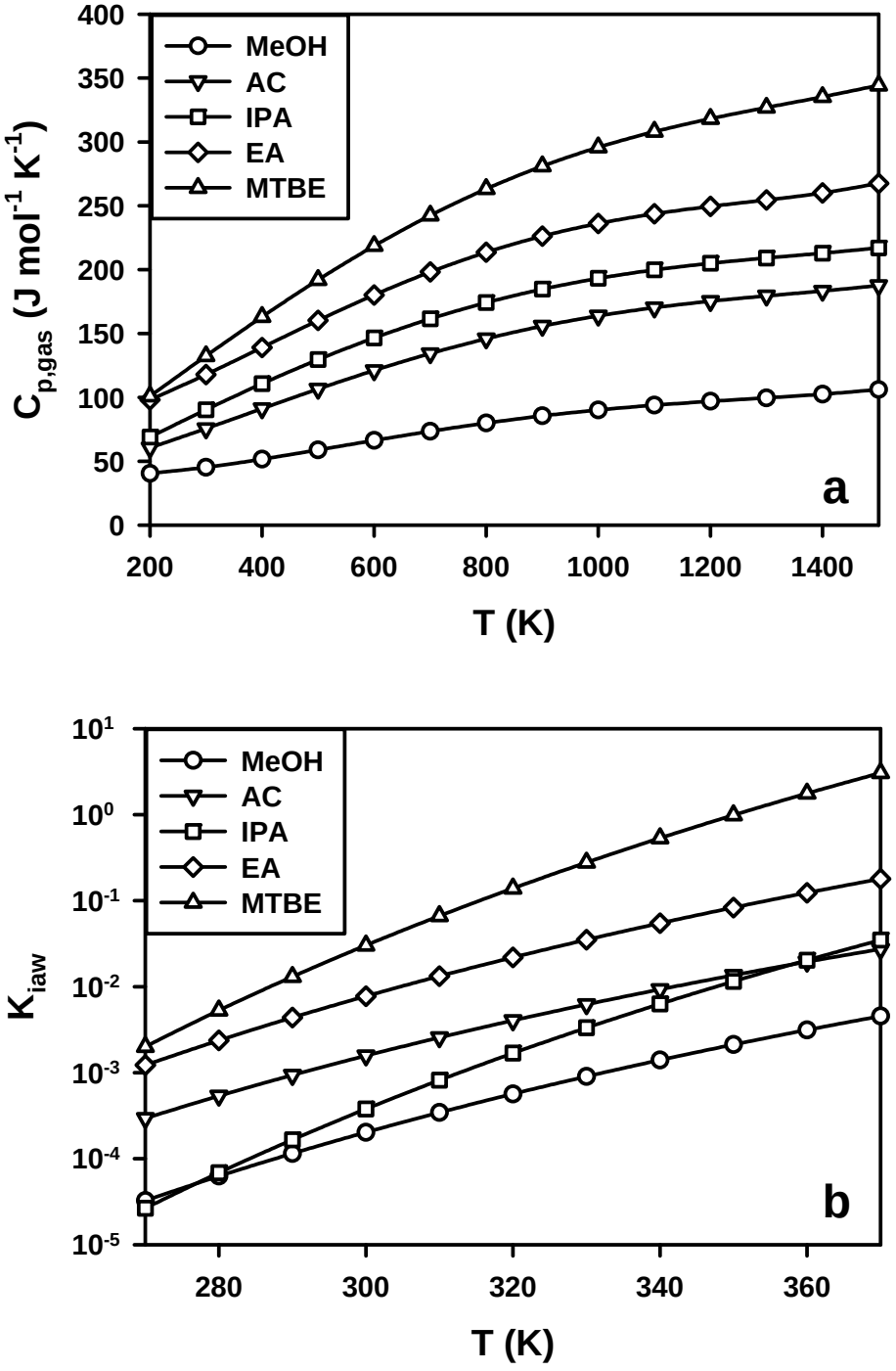

Figure 6.10. The LC/MS calibration curves for PFOS (a) and PFOA (b) from 1 to 200 ppb.